Journal of Alloys and Compounds 686 (2016) 693–701

Contents lists available at ScienceDirect

Journal of Alloys and Compounds

journal homepage: http://www.elsevier.com/locate/jalcom

Dissimilar friction stir welding of 6061 Al to 316 stainless steel using Zn as a filler metal

Qixian Zheng, Xiaomei Feng, Yifu Shen*, Guoqiang Huang, Pengcheng Zhao

College of Materials Science and Technology, Nanjing University of Aeronautics and Astronautics (NUAA), Yudao Street 29, 210016 Nanjing, PR China

ARTICLE INFO

Article history:
Received 30 January 2016
Received in revised form
3 June 2016
Accepted 9 June 2016
Available online 11 June 2016

Keywords:
Friction stir welding
Dissimilar welding
Lap joints
Macro and microstructure

ABSTRACT

The need of jointing aluminum and steel is increasing in automobiles industry. The FSW has advantages over fusion welding in dissimilar welding, and studies about FSW of aluminum and steel has been reported widely. However, FSLW of aluminum and steel using Zn as filler metal is few. In this study, sound Al–Zn-steel "sandwich" joints were achieved. With the tool pin inserted into zinc foil, vast zinc was stirred into aluminum fabricating Al–Zn mixing layer structure in the upper part of aluminum side. Thin steel-Zn mixing layer structure was discovered at the interface. No intermetallic compound interlayer was discovered at the interface. The lap joints with zinc foil as filler metal showed better strength than joints without filler metal. The microstructure of joints and the effect of Zn foil thickness on the joint strength were discussed.

1. Introduction

There is a clear trend in manufacturing automobiles toward the combination of aluminum alloy and steel to satisfy the purpose of reducing the weight of automobiles to improve fuel efficiency and energy preservation [1]. The jointing aluminum alloy and steel was recognized as a challenge due to the huge difference in chemical and physical properties of them. Resulting from the large difference in thermal expansion between aluminum alloy and steel, fusion welding would introduce large residual stress, not to mention the brittle intermetallic compound (IMC) would be inevitably formed at the joint [2]. Friction stir welding (FSW), a solid state joining technique panted by The Welding Institute in 1991 [3] has emerged as an innovative and promising welding process. FSW offers many advantages in the suppression of defects such as blow holes, segregation, cracks and generation of IMC, compared with traditional fusion welding [4]. These attractive advantages make FSW intensively used in dissimilar welding [5–9] and studies published on the FSW of Al to steel in butt joint and lap joint are in a considerable number. Xiong JT [10] fabricated the lap joints of aluminum and stainless steel by FSW with cutting pin. Formation of the macro-interlocks resulting from the steel flashes plugging into the upper aluminum at both sides of the nugget bottom and the mechanical bonding of micro interlocks were formed at the aluminum/steel interface. Brittle IMC layer ($FeAl_3$) was discovered at the joining interface. EDS analysis revealed that fracture surface was covered by a thin aluminum layer and IMC. Ramachandran KK et al. [11] investigated the effect of tool axis offset and geometry of tool pin profile on the characteristics of friction stir welded butt joints of aluminum and HSLA steel. Under a given parameter, a best joint with a joint strength of 188 MPa was obtained with specific taper angle of the taper cylindrical tool pin and axis offset. IMC layer (Al_5Fe_2, FeAl, $FeAl_3$) was discovered at the joining interface and a blend of brittle and ductile fracture occurred at the interface. In addition to these, numerical simulation was employed to optimize the Al/steel FSW [12]. There is a fact we can't ignore that even though successful FSW of Al/steel have been achieved and thick interlayer composed of brittle IMC were avoided, joint interface still exist a mass of brittle IMC such as FeAl, Al_5Fe_2 and $FeAl_3$ [10–13], which could result in brittle fracture.

Al/Cu FSW also face the problem of generating IMC layer [7–9]. To avoid this problem, Kuang BB et al. [14] used Zn foil as filler metal to carry out friction stir lap welding (FSLW) of Al to pure Cu, as both Al and Cu could form alloys with Zn according to the phase diagram. The report about dissimilar FSW of Al to steel using Zn foil as filler metal is few. According to the Zn–Fe phase diagram, Zn and steel could generate intermetallics [15]. Yang J et al. [16] added Zn to the fusion zone of the Al/steel joint which was achieved by laser welding. Due to the addition of the Zn, the IMC in the Al/steel joint changed from the layered Fe_2Al_5 and needle-like $FeAl_3$ to layered

* Corresponding author.
E-mail address: yfshen_nuaa@hotmail.com (Y. Shen).

http://dx.doi.org/10.1016/j.jallcom.2016.06.092
0925-8388/

$Fe_2Al_{5-x}Zn_x$ and dispersed $FeZn_{10}$ with minor Al rich amorphous phase. The joint with Zn addition manifested a significant improvement of the joint strength, compared with the joint without Zn addition. The reason for this effect is that $FeZn_{10}$ has lower hardness and brittleness than FeAl, Al_5Fe_2 and $FeAl_3$. Improvement of the strength of the Al/steel lap joint fabricated by FSLW with Zn as filler metal stand a good chance, due to the $FeZn_{10}$ reveals low hardness and brittleness. Using filler metal in lap joints compose “sandwich structure”, which is familiar in the field of dissimilar materials brazing [17]. The melted filler metal with low melt temperature would form reaction layer with base material at high temperature. In this way, the dissimilar materials realize firm jointing without contact. In the field of dissimilar alloy FSLW, plunge depth plays a vital role in the joint strength. Inserting the tool pin into soft alloy could avoid the severe wear of the tool, while a slight difference in plunge depth has a significant effect on the performance of the lap joints [18]. Plunging part of the pin into hard alloy can enhance the joint strength, however if the plunge depth is too large, the pin wears out in a short time with the aluminum burned [19]. To solve this dilemma, a wear resistant welding tool is necessary. In another way, the addition of the filler metal in this experiment may change this situation as the Zn foil could melt without inserting welding tool into it [14].

The objective of this study is to obtain sound lap joints of Al/steel by FSLW with Zn as filler metal from various welding parameters (rotation speed and traverse speed) under the given plunge depth. The effect of the welding parameters (thickness of the Zn plate and depth of tool pin intruding into steel) on the mechanical properties would be investigated. Microstructure of the interface of joints and the interlayer at the interface would also be discussed.

2. Experimental procedures

The materials employed in this study were 6061 aluminum alloy, 316 stainless steel and pure Zn foil. The chemical composition of these materials was listed in Table 1. All of these alloys were received as plates.

All the sheets were degreased with methanol solvent after light sanding of plates to remove oxide and impurities. The steel was placed at the bottom, the aluminum was placed at the topside and the Zn foil was placed between them, which composed “sandwich structure” as shown in Fig. 1a. Welding tool made of WC-13%Co was employed with a diameter of 18 mm shoulder and 1.5 mm long for the threaded conical pin which was tapered from the root diameter of 5 mm to the top diameter of 4 mm. The long term served welding tool was displayed in Fig. 1b, no severe wear occurred with some blend of zinc and aluminum attached. Steel plates were employed with constant thickness of 2 mm. To investigate effect of the thickness of Zn foil on the properties of the lap joint, different thicknesses of Zn foil (0.1 mm and 0.3 mm) were adopted. Considering the length of the tool pin was 1.5 mm, various thicknesses (1.2–1.7 mm) of Al sheets were accepted. After a series of experiments, a constant rotation speed (1200 rpm), traverse speed (40 mm/min), plunge depth (0.1 mm) and welding tool title angle of 2° was employed. Detailed parameters and thickness of Zn foil and Al plate were listed in Table 2. The plunge depth means depth of shoulder plunging into Al plate, while insert depth means depth of tool pin inserting into steel plate. To monitor thermal history of interface under various process conditions, K-type thermocouple was embedded underneath the interface as illustrated in Fig. 1a (0.2 mm from steel surface).

Table 1
The chemical composition of the employed materials (mass fraction %).

Material	Element							
316 Steel	C	Si	Mn	P	S	Ni	Cr	Mo	Fe
Fraction	0.08	1.00	2.00	0.02	0.02	12	17	2	bal
6061 Al	Cu	Si	Fe	Mn	Mg	Zn	Cr	Ti	Al
Fraction	0.2	0.6	0.7	0.15	0.9	0.25	0.1	0.15	bal
Zn foil	Zn								
Fraction	99								

After being mechanically polished, microstructure and shape of cross section of weld joints were observed by optical microscopy. More delicate structure and chemical compositions of interlayer were analyzed utilizing the scanning electron microscope (SEM). The fracture surfaces of lap joints were tested via X-ray diffraction (XRD) pattern. Vickers microhardness and failure load value (KN) were utilized to evaluate mechanical properties of FSW samples at ambient temperature. The microhardness of cross section of weld joints was measured parallel to the interface using an HXS-1000 microhardness tester with a load of 9.8 N and dwell time of 15 s. The Al side and steel side were both tested parallel to the joint interface. Considering the FSW had limited influence on steel, Al plate was tested at the center while steel was tested at 0.1 mm away from interface. The ultimate result was averaged by a set of five data tested under each process condition. To make the shear strength precise, three shear test specimens were made as displayed in Fig. 1c and tested at a rate of 2 mm/min using an Instron-5581 electromechanical testing machine at room temperature.

3. Results and discussion

3.1. Macrograph of the surface of lap joints

Classic defects of FSW such as groove, furrow, hole could be observed in Fig. 2a and b when the welding parameters beyond the suitable one. Sample in Fig. 2a was obtained under the parameter of 600 rpm, 40 mm/min, 0.1 mm and sample in Fig. 2b was obtained under the parameter of 900 rpm, 40 mm/min, 0.1 mm. Reasons for the defects on the surface of samples in Fig. 2a and b are simple. Rotation speeds of 600 rpm and 900 rpm are too low to generate enough heat to maintain the aluminum at the excellent state of thermoplasticity, which led to the Al alloy couldn’t fill the cavity left by rapid rotary welding tool well. After a series of experiments, sound surface of lap joints were achieved under process condition No.1~6 as displayed in Fig. 2c.

3.2. Thermal histories

Fig. 3 gives the real-time temperature changing curves of process condition No.1-5 recorded by K-type thermocouple positioned at steel plate. The peak temperatures of process condition No.2-5 during FSW were all higher than the melting point of Zn, while the peak temperature of process condition No.1 during FSW was lower than it. Low peak temperature of process condition No.1 resulting from no friction at interface. With tool pin insert into steel, process condition No.3 and No.5 manifested higher peak temperature. Under process condition No.2-5, the time of temperature higher than the melting point of Zn could last 10–20 s. In this circumstance, Zn foils would melt without doubt and in good state of fluidity. It’s not hard to see that tight conjunction of “sandwich structure” would form after Zn foils being solid as the rapid rotary tool would make melted Zn perform good contact with Al and steel. Owing to “sandwich structure”, Al and steel wouldn’t contact, which avoid the formation of IMC between Al and Fe at high temperature.

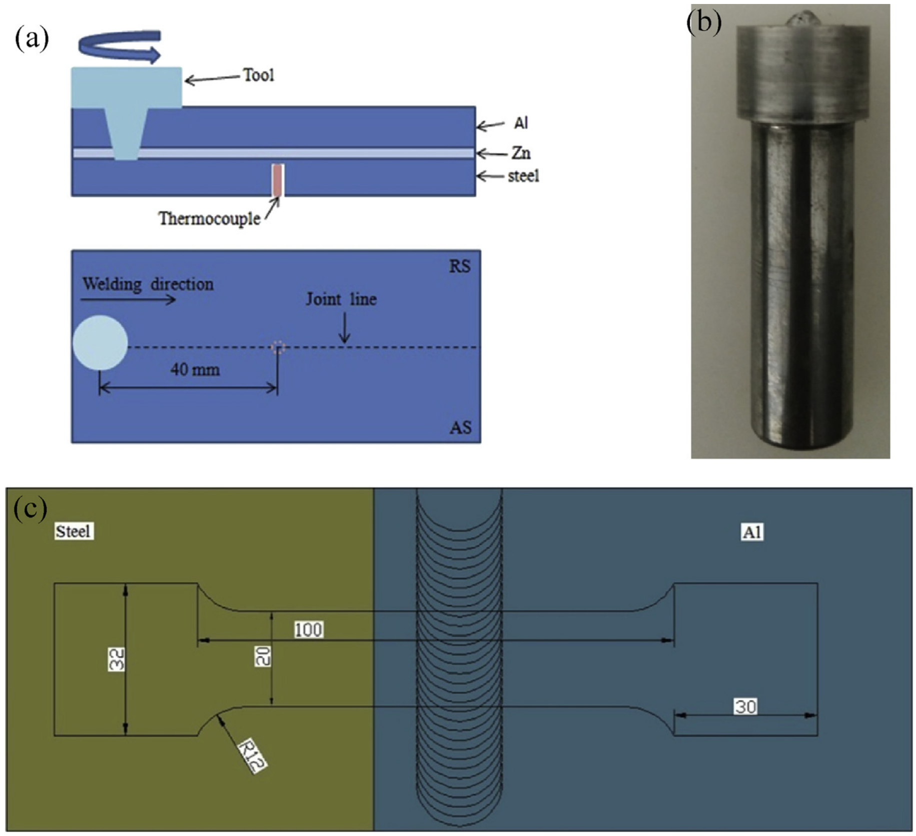

Fig. 1. Experiment setup: (a) FSLW setup, (b) long term serviced welding tool, (c) construction of specimen for shear test.

Table 2
Welding parameters and thicknesses of Zn foils and Al plates.

Process condition no.	Rotation speed (rpm)	Travers speed (mm/min)	Zn thickness (mm)	Al thickness (mm)	Plunge depth (mm)	Insert depth (mm)
1	1200	40	0.1	1.7	0.1	0
2	1200	40	0.1	1.5	0.1	0
3	1200	40	0.1	1.4	0.1	0.1
4	1200	40	0.3	1.3	0.1	0
5	1200	40	0.3	1.2	0.1	0.1
6	1200	40	0	1.5	0.1	0.1

3.3. *Macrograph and microstructure of the cross section of the joints*

During preparation of samples for the observation of cross section of joints, the joint under process condition No.1 was separated. As displayed in Fig. 4, Al side attached with Zn foil while Zn foil didn't remain on the steel side. As the process condition listed in Table 2, the tool pin didn't touch the Zn foil. Heat during the FSW process come from the friction between welding tool and aluminum, which was not enough to melt all the Zn foil as indicated from Fig. 3 but the topside of the Zn foil may melted. Due to that, metallurgical bonding generated between Al and Zn but steel and Zn. In consequence, the process condition No.1 wouldn't be discussed. The joint under process condition No.6 was used to compare the shear strength with joints under process condition No.2~5, so the process condition No.6 wouldn't be discussed either.

Fig. 5 reveals the cross section of the joint under process condition No.2. Due to that the tool pin didn't insert into steel, the interface was in straightness, no hook formed. A 2 μm interlayer was observed at the interface as shown in Fig. 5b and no defect was detected. The 2 μm interlayer could also be found in joints under process condition No.3-5.

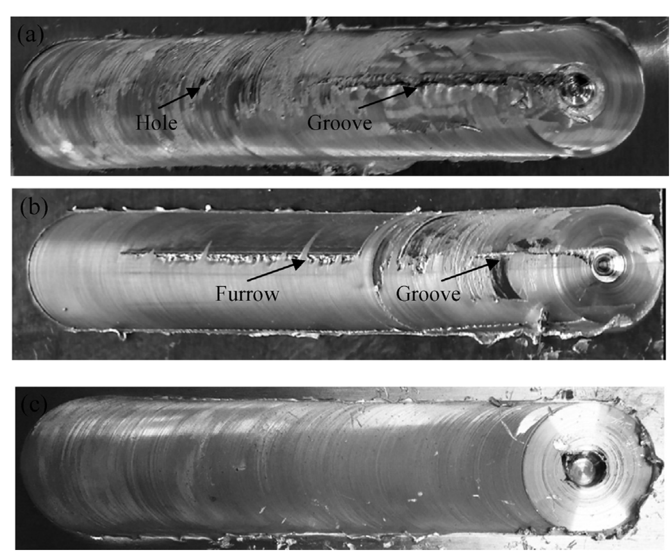

Fig. 2. Macrograph of the surface of lap joints under various parameters: (a) 600 rpm, 40 mm/min, 0.1 mm; (b) 900 rpm, 40 mm/min, 0.1 mm; (c) 1200 rpm, 40 mm/min, 0.1 mm.

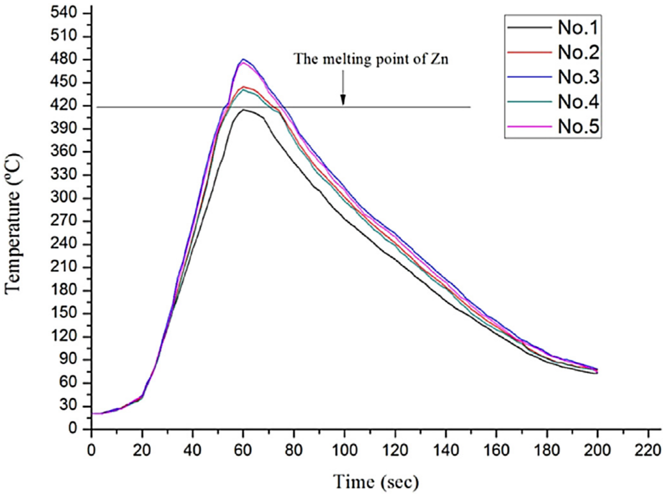

Fig. 3. Thermal histories of different process conditions.

The cross section of the joint under process condition No.3 was showed in Fig. 6. In this process condition, the tool pin was inserted into steel side, which resulted in the formation of hooks at the interface. In another way, the hooks composed the macro-interlock structure, which is beneficial to the joint strength. Several steel particles distributed uniformly in steel side as shown in Fig. 6a and steel particles were covered by Zn foil as shown in Fig. 6b which indicated the Zn was melted during the welding process. Considering the “sandwich” FSW setup, it’s not hard to figure out this phenomenon. As the tool pin inserted into the steel, part of the melted Zn was stirred into steel, which formed the steel-Zn mixed layer structure at the interface as displayed in Fig. 6c. Clearly this structure has positive influence on the joint strength.

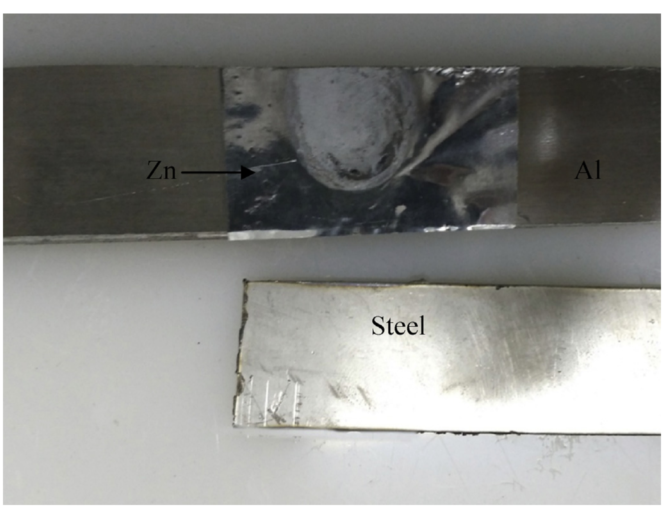

Fig. 4. Separate parts of the joint under process condition No.1.

Cross section of the joint under process condition No.4 is displayed in Fig. 7. Zn was in streamline in Al side and vortex flow could be found, which indicated large amount of Zn was melted and was stirred into Al side. The aluminum was softened by the rapid rotary tool pin meanwhile the melted Zn was stirred into softened aluminum. Under this complicated situation, Al–Zn mixed layer was formed as revealed in Fig. 7b. There existed downward force from the welding tool during the FSW process, which contributed to the softened aluminum stirred into the Zn foil. As shown in Fig. 7c, complicated Al–Zn mixed layer was adjacent to the interface. The obvious white zone close to the retreating side (RS) is the unmelted Zn foil in the process. The melted Zn foil surrounding the rotary tool pin, in another word, between the uninfluenced Zn foil and hook, was squeezed to unmelted Zn foil by pressed aluminum. Temperatures in the FSW process, a unique feature, generally speaking is the presence of asymmetry in the temperature of each side of the weld joint [20]. The temperature of advancing side (AS) is usually higher than that of retreating side [20], which contributed to the fact that much more Zn foil was squeezed in advancing side than that in retreating side.

Cross section of the joint under process condition No.5 is shown in Fig. 8. Some similar phenomenon, Al–Zn mixed layer structure in Al side and Zn-steel mixed layer structure at the interface, could be observed. The unique feature was that steel particles were between the Al–Zn mixed layer as manifested in Fig. 8b and c. In another hand, a hole could be discovered at the advancing side as revealed in Fig. 8a. The stirred steel particles resulting from the speed rotary tool pin may contribute to the generation of the hole. The particles displayed in Fig. 8b were at the upper part of the Al side, which indicated that there existed sufficient flow in the stir zone.

3.4. Element diffusion

The SEM image of the joint interface under process condition No.2 was showed in Fig. 9a. The light side was steel, and the dark side was Zn and aluminum. No interlayer was found between steel and Zn which was not discovered at joint interface under process condition No.3-5 either. The corresponding energy dispersive spectrometer (EDS) line result was showed in Fig. 9b. The element diffusion zone (EDZ) could be discovered from the EDS line result, which could be found at joint interface under process condition No.3-5 as well. The width of the element diffusion zone for each process condition was revealed in Fig. 9c. The tool pin was inserted into steel under the No.3 and No.5 process condition, which would generate more heat than that under No.2 and No.4 process

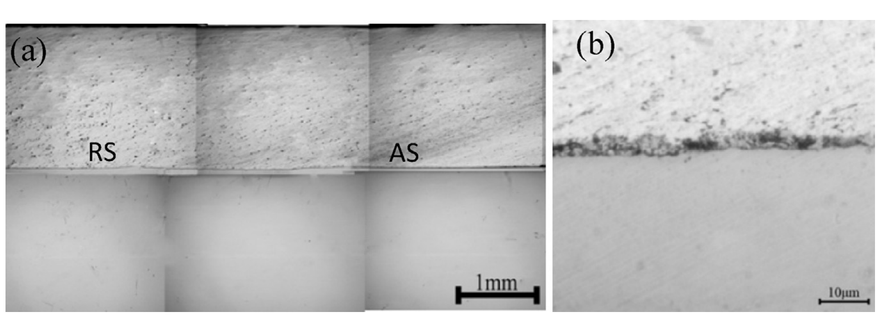

Fig. 5. Cross section of the joint under process condition No.2: (a) overview; (b) enlarged view of interface.

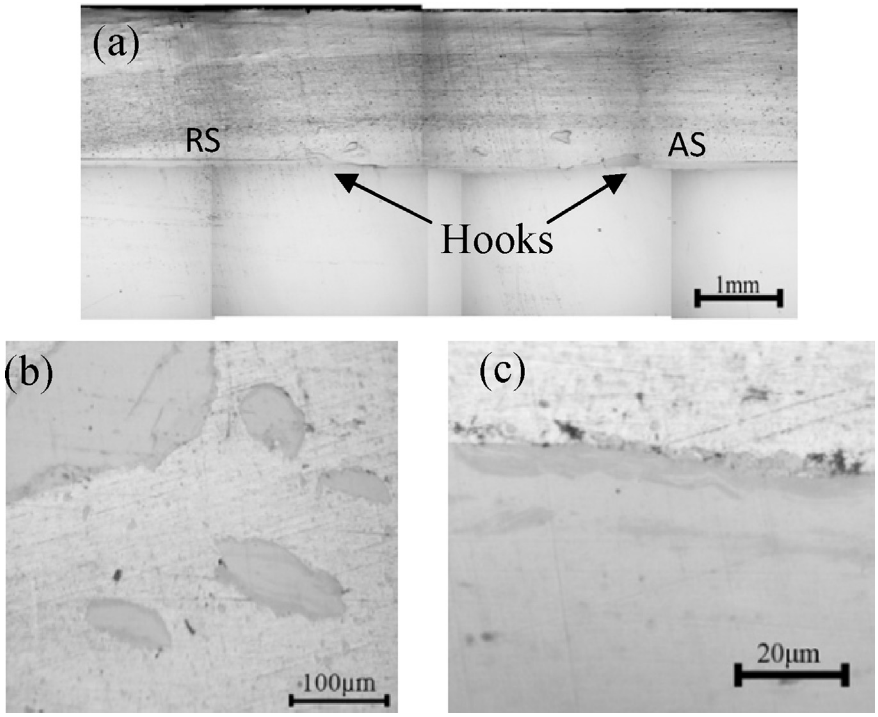

Fig. 6. Cross section of the joint under process condition No.3: (a) overview; (b) steel particles covered by zinc; (c) steel-Zn mixed layer structure.

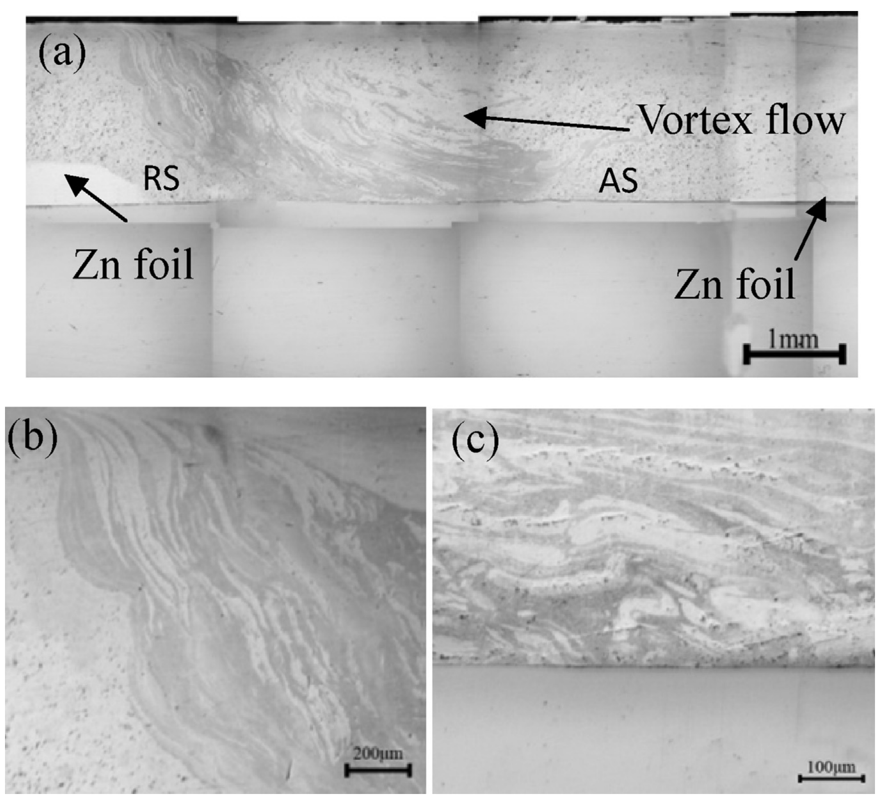

Fig. 7. Cross section of the joint under process condition No.4: (a) overview; (b)Al–Zn mixed layer; (c) Al–Zn mixed layer at the interface.

condition. Clearly, the more the heat generated, the wider the element diffusion zone in steel side. The EDS quantitative analysis results of the local regions in dark side were listed in Table 3. According to the Zn–Fe phase diagram, a little $FeZn_{10}$ may be generated as no obvious interlayer generated between Zn foil and steel. In steel side adjacent to interface, solid solution of zinc in iron (Fe(Zn)) was generated according to the EDS quantitative analysis result. The element diffusion indicated the firm metallurgical bond

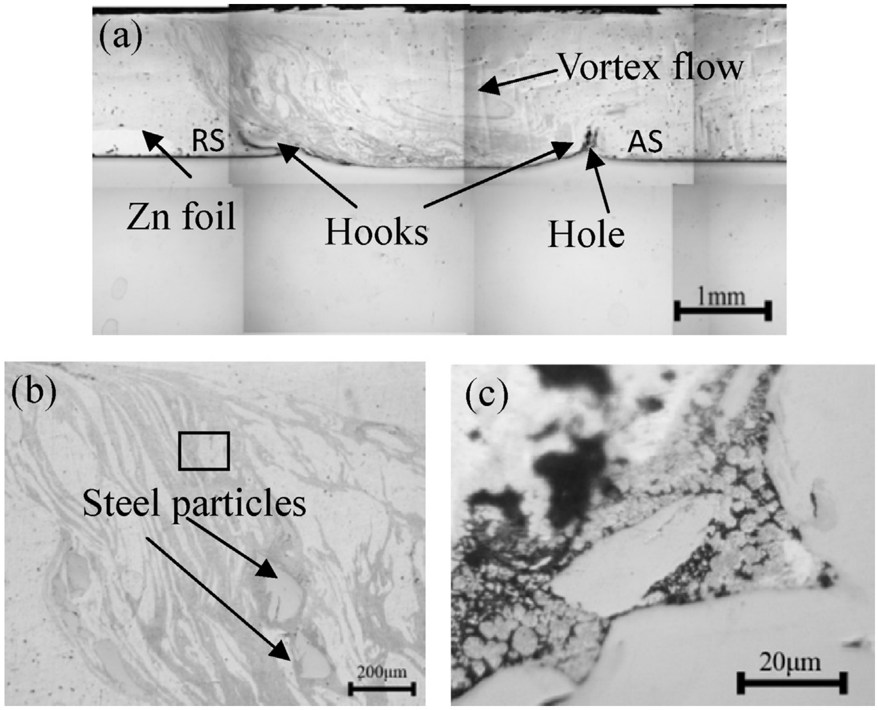

Fig. 8. Cross section of the joint under process condition No.5: (a) overview; (b) steel particles between Al–Zn mixed layer; (c) steel particles in Al–Zn mixed layer at the interface.

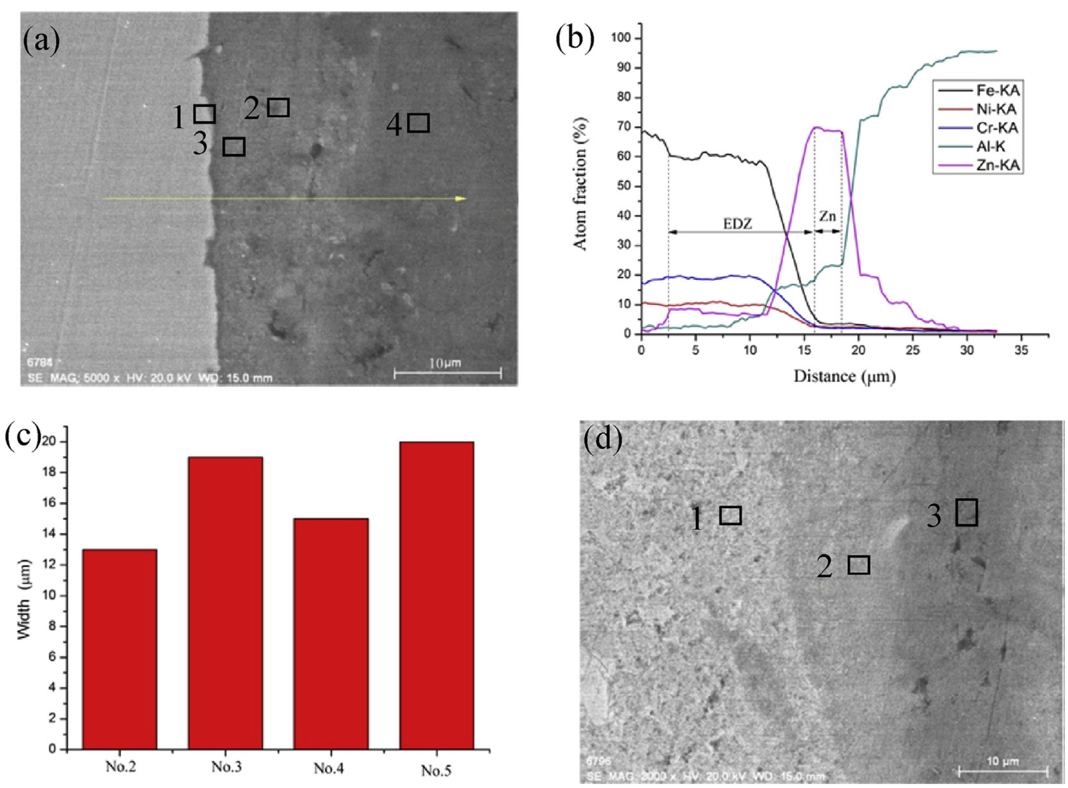

Fig. 9. Element diffusion: (a) SEM image of No.2 interface; (b) EDS line result; (c) width of EDZ of joints under process condition No.2-5; (d) SEM image of local region in Fig. 8b.

between Zn foil and steel. Fig. 9d revealed the SEM image of the marked local region in Fig. 8b, where is the Al–Zn mixed layer structure. The EDS quantitative analysis results as listed in Table 4 revealed that solid solution of aluminum in zinc (Zn(Al)) and solid solution of zinc in aluminum (Al(Zn)) were generated according to the Al–Zn diagram. These phenomena (EDZ, solid solutions) could also be found in other process conditions.

Table 3
EDS quantitative analysis results of the points in Fig. 9a (atom fraction %).

Element	Fe	Zn	Ni	Cr	Al
1	69.91	2.01	10.67	17.41	–
2	5.45	91.52	–	–	3.03
3	8.45	85.24	–	–	6.31
4	0.57	8.98			90.45

Table 4
EDS quantitative analysis results of the points in Fig. 9d (atom fraction %).

Points	1	2	3
Al	34.77	68.42	70.23
Zn	65.23	31.58	29.77

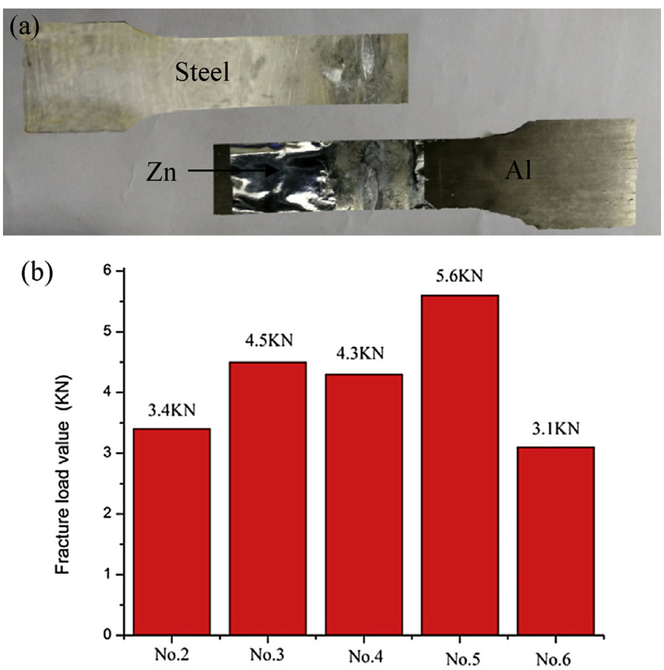

Fig. 10. Shear test: (a) macrograph of fracture surface; (b) fracture load value of joints. under process condition No.2-6.

3.5. Mechanical properties

3.5.1. Shear strength

The failure load of lap joints was chosen to evaluate the joint strength. A series of shear testing were carried out utilizing specimens extracted from No.2-6 as shown in Fig. 1c. To make the result precise, ultimate shear testing results were averaged by five set of data from each process condition. Every specimen was fractured at the interface as shown in Fig. 10a. The fracture load values of various FSW process conditions were manifested in Fig. 10b. The minimum joint strength was achieved at the process condition No.6, which indicated that the addition of the Zn foil did improve the joint strength. The improvement of the joints strength could attribute to the firm metallurgical bonding between the Zn foil and steel. Comparing the process condition No.2 with No.4 (or the process condition No.3 with No.5), more Zn foil participated in the FSW process, which enlarge the element diffusion zone in steel side. It's not hard to draw the conclusion that wider element diffusion zone would make the metallurgical bonding tighter and improve the joint strength. Comparing the process condition No.4 with No.5 (or the process condition No.2 with No.3), apparent increase of joint strength could be discovered. With the tool pin inserting into steel, macro-interlock structure composed of the hooks at advancing side and retreating side respectively was formed and element diffusion zone was enlarged due to more heat generated. Apparently, effect of macro-interlock and enlarged element diffusion zone contributed to the increase of the joint strength.

To identify if there were intermetallic phases on fracture surfaces, the fracture surfaces on steel side of joints under process condition No.3 and No.5 were analyzed via XRD patterns as can be seen in Fig. 11. The XRD patterns indicated that no intermetallic phase was detected, but Fe(Zn), Al(Zn) and Zn(Al) were detected. Comparing the process condition No.3 with No.5 XRD patterns, less zinc peak was found in XRD pattern for process condition No.5, which indicated that more Fe(Zn) and Al(Zn) was generated.

The SEM images of fracture surface of the lap joints were displayed in Fig. 12. Fig. 12a–d were fracture surfaces of steel side under process condition No.2-5 respectively. EDS quantitative analysis results of marked local regions were listed in Table 5. As shown in Fig. 12a the joint under process condition No.2 fractured at Zn foil (light part) where adhere to steel resulting from metallurgical bonding. Some aluminum (gray part) was attached with the Zn foil. From the enlarged view of the aluminum, dimples which are the typical character of the ductile fracture could be

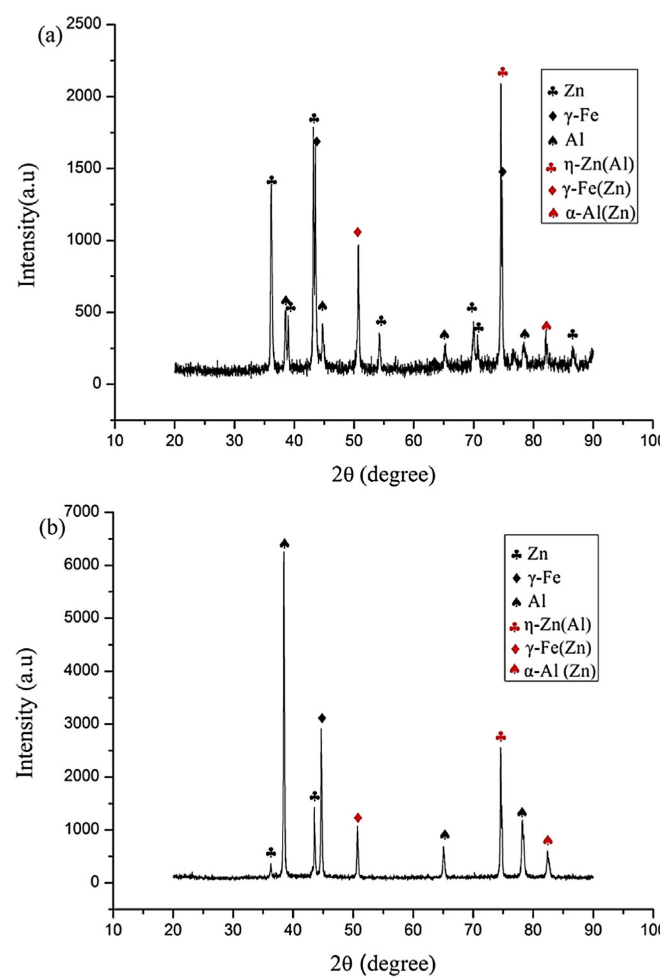

Fig. 11. XRD patterns of fracture surfaces on steel side under process condition: (a) No. 3; (b) No. 5.

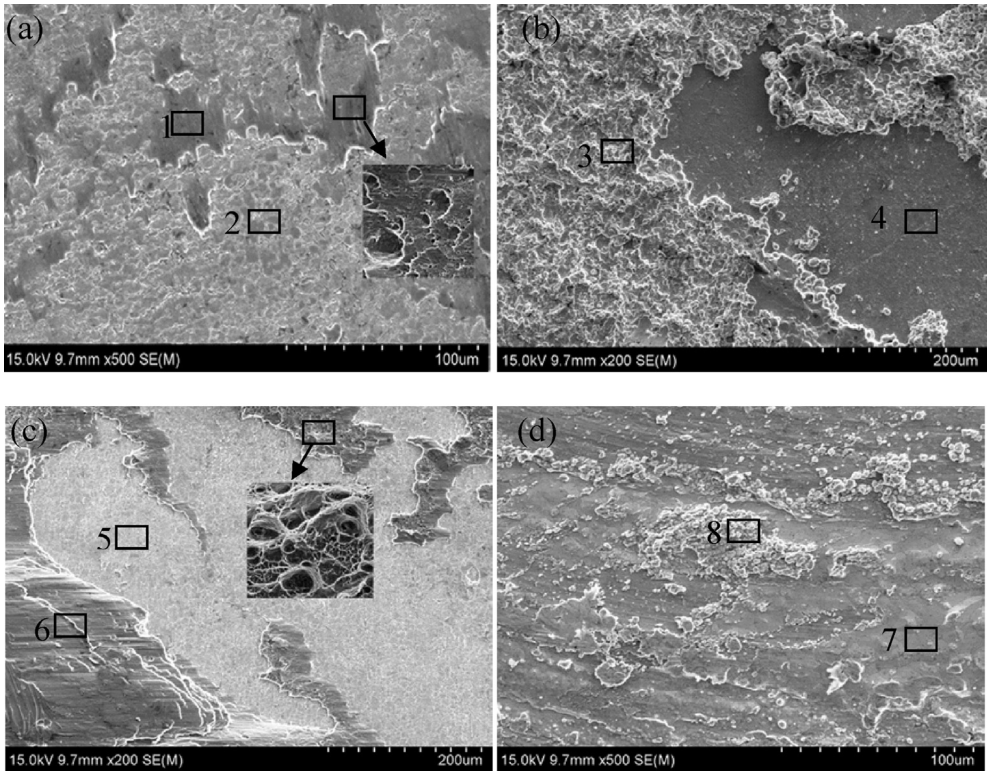

Fig. 12. SEM images of fracture surface of steel side under process condition: (a) No. 2; (b) No. 3; (c) No 4; (d) No. 5.

Table 5
EDS quantitative analysis results of the points in Fig. 12 (atom fraction %).

Element	Fe	Zn	Ni	Cr	Al
1	–	2.01	–	–	97.99
2	–	97.51	–	–	2.49
3	–	85.24	–	–	14.76
4	69.37	3.04	10.74	16.85	–
5	–	95.78	–	–	4.22
6	–	3.18	–	–	96.82
7	–	98.23	–	–	1.77
8	–	83.76	–	–	16.24

found. The fracture surface of the joint under process condition No.4 had the similar situation as displayed in Fig. 12c. According to EDS quantitative analysis results, the flat part in Fig. 12b was steel while the other part was Zn and Zn(Al). The fracture surface under process condition No.5 was Zn(Al) on the Zn foil according to EDS quantitative analysis results.

3.5.2. Microhardness

Microhardness of lap joints were tested parallel along the interface. Due to the recrystallization [18] and the generation of solid solutions, stir zone in both sides expressed with higher hardness. Resulting from more zinc involved in FSW process, which means more solid solutions was generated, Al side under process

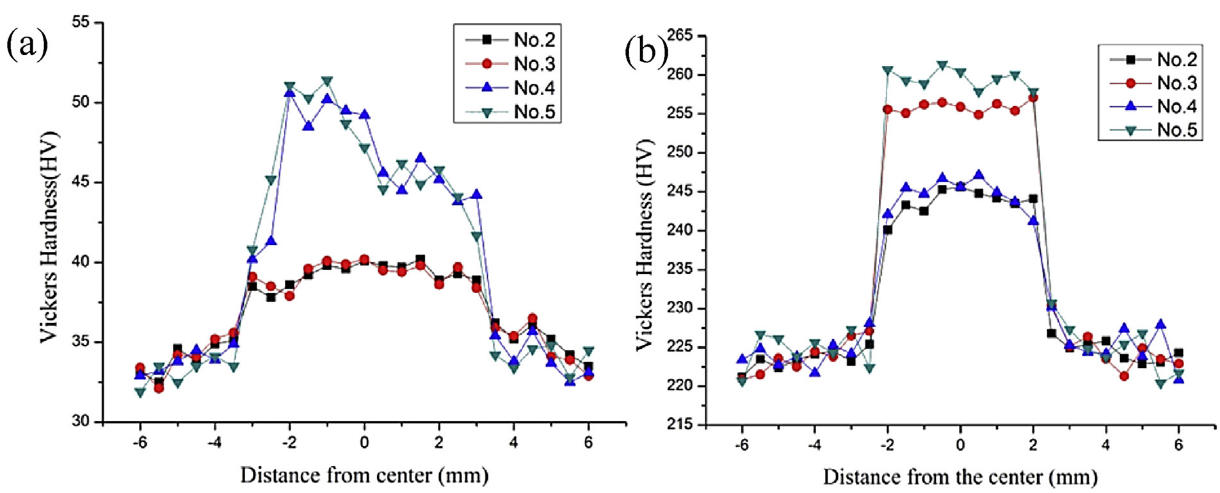

Fig. 13. Vickers hardness of cross section of joints under process condition No.2-5: (a) aluminum side; (b) steel side.

condition No.4 and No.5 manifested higher hardness than joints under process condition No.2 and No.3 as shown in Fig. 13a. It should be noted that retreating side in process condition No.4 and No.5 on Al side had more zinc that retreating side displayed higher hardness than advancing side.

The insertion of tool pin into steel side would introduce more heat which would promote recrystallization in steel side and the generation of Fe(Zn). In consequence, on steel side, the process condition No.5 displayed the maximum hardness and process condition No.3 manifested higher hardness than process condition No.2 and No.4 as shown in Fig. 13b.

4. Conclusion

1. Sound lap joints with "sandwich structure" were achieved in this study.
2 Vast zinc was stirred into aluminum and manifested in streamline under process conditions of No.4 and No.5. It should be noted that more zinc is found in retreating side than that in advancing side.
3. According to the EDS quantitative analysis, a little $FeZn_{10}$ may be generated but no IMC interlayer generated when the tool pin inserted into zinc foil.
4. Macro-interlocks, Al–Zn mixed layer and Zn-steel mixed layer have good influence on joint strength, and the maximum strength was achieved under process condition No.5.
5. Various solid solutions were detected via XRD patterns from the fracture surfaces of the lap joints.

Acknowledgements

The study work of this paper is supported by the National Natural Science Foundation of China (Grant No. 51475232).

This is a project funded by the Priority Academic Program Development of Jiangsu Higher Education Institutions (PAPD).

References

[1] E. Schubert, M. Klasen, I. Zerner, C. Walz, G. Sepold, Light-weight structures produced by laser beam joining for future applications in automobile and aerospace industry, J. Mater. Process. Technol. 15 (2001) 2–8.
[2] J.B. Sun, Q. Yan, W. Gao, J. Huang, Investigation of laser welding on butt joints of Al/steel dissimilar materials, Mater. Des. 83 (2015) 120–128.
[3] W.M. Thomas, E.D. Nicholas, J.C. Needham, M. G. Murch, P. Temple Smith, C. J. Dawes. Friction stir butt welding. International patent application No. PCT/GB92/02203; December 1991.
[4] R.S. Mishra, Z.Y. Ma, Friction stir welding and processing, Mater. Sci. Eng. R. 50 (2005) 1–78.
[5] Y.N. Wei, J.L. Li, J.T. Xiong, F. Huang, F.S. Zhang, S.H. Raza, Joining aluminum to titanium alloy by friction stir lap welding with cutting pin, Mater. Charact. 71 (2001) 1–5.
[6] B. Li, Y.F. Shen, L. Luo, W.Y. Hu, Effect of processing variables and heat treatments on Al/Ti-6Al-4V interface microstructure of bimetal clad-plate fabricated via a novel route employing friction stir lap welding, J. Alloy Compd. 658 (2016) 904–913.
[7] M. Akbari, P. Bahemmat, M. Haghpanahi, M.B. Givi, Enhancing metallurgical and mechanical properties of friction stir lap welding of Al-Cu using intermediate layer, Sci. Technol. Weld. Joi. 18 (2013) 518–524.
[8] T. Saeid, A. Abdollah-zadeh, B. Sazgari, Weldability and mechanical properties of dissimilar aluminum-copper lap joints made by friction stir welding, J. Alloy Compd. 490 (2010) 652–655.
[9] P. Xue, B.L. Xiao, D.R. Ni, Z.Y. Ma, Enhanced mechanical properties of friction stir welded dissimilar Al-Cu joint by intermeallic compounds, Mater. Sci. Eng. A Struct. 527 (2010) 5723–5727.
[10] J.T. Xiong, J.L. Li, J.W. Qian, F.S. Zhang, W.D. Huang, High strength lap joint of aluminium and stainless steels fabricated by friction stir welding with cutting pin, Sci. Technol. Weld. Join. 17 (2012) 196–201.
[11] K.K. Ramachandran, N. Murugan, S. Shashi Kumar, Effect of tool axis offset and geometry of tool pin profile on the characteristics of friction stir welded dissimilar joints of aluminum alloy AA5052 and HSLA steel, Mater. Sci. Eng. A Struct. 639 (2015) 219–233.
[12] X. Liu, S.H. Lan, J. Ni, Electrically assisted friction stir welding for joining Al 6061 to TRIP 780 steel, J. Mater. Process. Technol. 219 (2015) 112–123.
[13] X. Liu, S.H. Lan, J. Ni, Analysis of process parameters effects on friction stir welding of dissimilar aluminum alloy to advanced high strength steel, Mater. Des. 59 (2014) 50–62.
[14] B.B. Kuang, Y.F. Shen, W.H. Chen, H.S. Xu, J.C. Gao, et al., The dissimilar friction stir lap welding of 1A99 to pure Cu using Zn as filler metal with "pinless" tool configuration, Mater. Des. 68 (2015) 54–62.
[15] X.P. Su, N.Y. Tang, J.M. Toguri, Thermodynamic evaluation of the Fe–Zn system, J. Alloy. Compd. 325 (2001) 129–136.
[16] J. Yang, Y.L. Li, H. Zhang, W. Guo, Y. Zhou, Control of interfacial intermetallic compounds in Fe–Al joining by Zn addition, Mater. Sci. Eng. A Struct. 645 (2015) 323–327.
[17] J.C. Feng, L.X. Zhang, Interface structure and mechanical properties of the brazed joint of TiC cermet and steel, J. Eur. Ceram. Soc. 26 (2006) 1287–1292.
[18] A. Elrefaey, M. Gouda, M. Takahashi, K. Ikeuchhi, Characterization of aluminum/steel lap joint by friction stir welding, J. Mater. Eng. Perform. 14 (2005) 10–17.
[19] T. Watanabe, K. Kimapong, Friction stir welding of aluminum alloy to steel, Weld. J. 83 (2004) 227S–282S.
[20] D. Lohwasser, Z. Chen, Friction Stir Welding, from Basics to Application, first ed., Woodhead, Cambridge, 2010.